

AWARD NUMBER: W81XWH-13-1-0149

TITLE: *“Real-Time Measurement of Host Bioenergetics During Mycobacterium Tuberculosis Infection”*

PRINCIPAL INVESTIGATOR: Adrie J.C. Steyn, Ph.D.

CONTRACTING ORGANIZATION: University of Alabama at Birmingham,  
Birmingham, AL 35294

REPORT DATE: May 2015

TYPE OF REPORT: Final

PREPARED FOR: U.S. Army Medical Research and Materiel Command  
Fort Detrick, Maryland 21702-5012

DISTRIBUTION STATEMENT: Approved for Public Release;  
Distribution Unlimited

The views, opinions and/or findings contained in this report are those of the author(s) and should not be construed as an official Department of the Army position, policy or decision unless so designated by other documentation.

REPORT DOCUMENTATION PAGE				Form Approved OMB No. 0704-0188	
Public reporting burden for this collection of information is estimated to average 1 hour per response, including the time for reviewing instructions, searching existing data sources, gathering and maintaining the data needed, and completing and reviewing this collection of information. Send comments regarding this burden estimate or any other aspect of this collection of information, including suggestions for reducing this burden to Department of Defense, Washington Headquarters Services, Directorate for Information Operations and Reports (0704-0188), 1215 Jefferson Davis Highway, Suite 1204, Arlington, VA 22202-4302. Respondents should be aware that notwithstanding any other provision of law, no person shall be subject to any penalty for failing to comply with a collection of information if it does not display a currently valid OMB control number. PLEASE DO NOT RETURN YOUR FORM TO THE ABOVE ADDRESS.					
1. REPORT DATE May 2015		2. REPORT TYPE Final		3. DATES COVERED 15 Aug 2013 - 15 Feb 2015	
4. TITLE AND SUBTITLE PROPOSAL TITLE: "Real-Time Measurement of Host Bioenergetics During Mycobacterium Tuberculosis Infection"				5a. CONTRACT NUMBER W81XWH-13-1-0149	
				5b. GRANT NUMBER	
				5c. PROGRAM ELEMENT NUMBER	
6. AUTHOR(S)  Adrie J.C. Steyn, Ph.D.  E-Mail: asteyn@uab.edu				5d. PROJECT NUMBER	
				5e. TASK NUMBER	
				5f. WORK UNIT NUMBER	
7. PERFORMING ORGANIZATION NAME(S) AND ADDRESS(ES)  University of Alabama at Birmingham, 701 20th Street South Birmingham, AL 35294-0001				8. PERFORMING ORGANIZATION REPORT NUMBER	
9. SPONSORING / MONITORING AGENCY NAME(S) AND ADDRESS(ES)  U.S. Army Medical Research and Materiel Command Fort Detrick, Maryland 21702-5012				10. SPONSOR/MONITOR'S ACRONYM(S)	
				11. SPONSOR/MONITOR'S REPORT NUMBER(S)	
12. DISTRIBUTION / AVAILABILITY STATEMENT  Approved for Public Release; Distribution Unlimited					
13. SUPPLEMENTARY NOTES					
14. ABSTRACT  The unique ability of <i>Mycobacterium tuberculosis</i> ( <i>Mtb</i> ) to persist in humans in a dormant, drug-resistant state, sometimes reactivating to cause tuberculosis (TB) decades after the primary infection, has puzzled scientists for years. This, together with the fact that more than one third of the world's population is latently infected with <i>Mtb</i> and the emergence of multi-drug resistant (MDR), extensively drug-resistant (XDR) and super XDR (S-XDR) <i>Mtb</i> strains constitutes a major challenge to global health. Surprisingly, very little is known about the precise mechanisms that <i>Mtb</i> uses to subvert host immune responses and there is an urgent need to apply new state-of-the-art tools to determine precisely how <i>Mtb</i> overcomes host defenses in order to establish a persistent infection. <i>For this purpose, we will apply a novel technology that, to the best of our knowledge, has not yet been used to examine any microbial species.</i> The application of this tool, <i>for the first time</i> , will reveal a wealth of previously <i>unknown, quantitative</i> information about the bacterial oxygen consumption rate (OCR), the extracellular acidification rate (ECAR) and reserve respiratory capacity (RRC). To date, critical information regarding <i>Mtb</i> bioenergetics is not available and represents a significant gap in our understanding of <i>Mtb</i> physiology. Secondly, real-time metabolic profiling of human macrophages infected with <i>Mtb</i> mutants will identify <i>key bacterial factors</i> that target <i>specific</i> components of the host ETC. Lastly, mycobacterial genes and pathways that modulate the bacterial and host bioenergetic state will be identified. These findings are expected to have an important <i>positive impact on our understanding of mycobacterial physiology</i> , which will result in the development of innovative approaches toward the containment and treatment of TB.					
15. SUBJECT TERMS None Listed					
16. SECURITY CLASSIFICATION OF:			17. LIMITATION OF ABSTRACT  UU Unclassified	18. NUMBER OF PAGES  19	19a. NAME OF RESPONSIBLE PERSON USAMRMC
a. REPORT U Unclassified	b. ABSTRACT U Unclassified	c. THIS PAGE U Unclassified			19b. TELEPHONE NUMBER (include area code)

## Table of Contents

	<u>Page</u>
1. Introduction.....	4
2. Keywords.....	4
3. Overall Project Summary.....	4
4. Key Research Accomplishments.....	16
5. Conclusion.....	16
6. Publications, Abstracts, and Presentations.....	17
7. Inventions, Patents and Licenses.....	19
8. Reportable Outcomes.....	19
9. Other Achievements.....	19
10. References.....	19
11. Appendices.....	none



**1. INTRODUCTION:** *Mycobacterium tuberculosis* (*Mtb*), the bacterium that causes human tuberculosis (TB) disease, is an extremely successfully pathogen owing to its ability to persist in humans in a dormant, drug-resistant state, sometimes reactivating to cause TB disease decades after the primary infection. *Mtb* dormancy, as well as the known limitations of current anti-TB drugs and their inability to act on dormant bacilli, underscore the need to use innovative tools to examine the bioenergetic mechanisms that allow *Mtb* to enter, maintain and emerge from a persistent state of infection. The purpose our proposed work is to establish a novel technology that can examine the bioenergetic profile of *Mtb*, as well as the bioenergetics of infected host cells in real-time. Once mycobacterial genes and pathways that modulate the bacterial and host bioenergetic state are identified, there is the promise that these components can be used as drug targets that may lead to novel therapeutic strategies to control persistent and drug-resistant *Mtb*.

**2. KEY WORDS:** tuberculosis, metabolism, flux analysis, bioenergetics, persistence, dormancy, immune, glycolysis, respiration, infection

**3. OVERALL PROJECT SUMMARY:** This Final Project Summary outlines the progress in addressing TASK 1 and TASK 2 as outlined in our original Statement of Work:

**TASK 1 (Months 1-12), To define the bioenergetic profile of wild type and genetically defined mutants of *Mtb*.** Materials and supply costs for the first year were \$10,042.

**Subtask 1a. To define the bioenergetic profile of wild type mycobacterial species *Mtb*, *M. bovis* BCG and *M. smegmatis*.** Briefly, in order to carry out this specific sub aim, actively growing (log-phase) cells of *M. tuberculosis* H37Rv, *M. smegmatis* (*Msm*) and *M. bovis* BCG were used to prepare single cell suspensions for seeding into special XF96 plates. We generated bioenergetic profiles by measuring cellular respiration, glycolysis rate, ATP turnover and reserve respiratory capacity in response to pharmacological modulators of glycolytic and oxidative energy metabolism provided as part of XF kits (see methods). To minimize experimental variations and ensure reproducibility, standardizations need to be carried out:

i) Determine the method of choice (centrifugation or chemical coating) to make bacterial cells efficiently adhere to the plate's surface. In polyethyleneimine mediated conjugation, an appropriate working concentration (the one that does not interfere with cellular metabolism and effect viability of the cells) will be determined. Viability of the cells will be ascertained using standard alamar blue assay.

Bioenergetic measurements on the XF96 Extracellular Flux Analyser require that the cells being analysed are adhered to the bottom surface for the XF96 cell culture microplate in a monolayer. For non-adherent mycobacteria this limitation can be resolved by using Cell-Tak™ Adhesive, a non-immunogenic polyphenolic protein preparation isolated from the marine mussel, or poly-D-lysine or polyethylenimine to adhere the bacilli in a monolayer. We investigated Cell-Tak™ and poly-D-lysine to adhere the mycobacteria to the XF96 cell culture microplate, and decided to continue with Cell-Tak™ due to more reproducible results. Using Cell-Tak™ we were able to successfully measure the oxygen consumption rate (OCR) and extracellular acidification rate (ECAR) of all the different mycobacterial strains investigated to date, which to the best of our knowledge is an original finding (Figure 1). This also shows that Cell-Tak™ does not discriminate between different mycobacterial cell wall compositions.

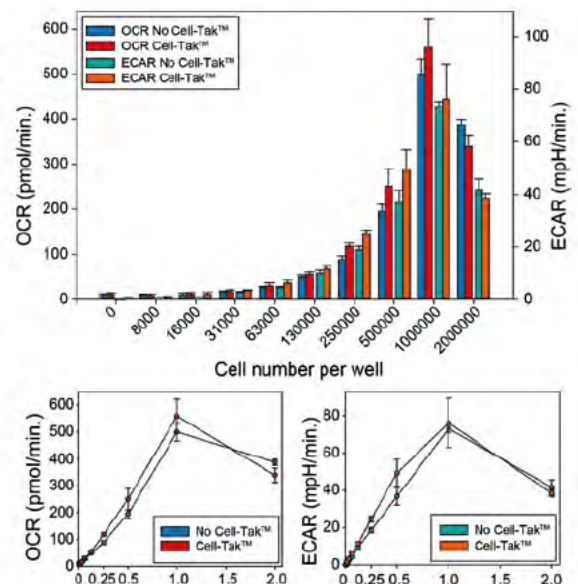


Figure 1: Bacilli seeding density optimization done with *Msm* on the XF96.



ii) Optimize seeding density for mycobacterial strains. Different species and cell types have different bioenergetic requirements. Hence for each species, appropriate seeding density needs to be optimized. This will require multiple sets of experiments and comparison of their cellular bioenergetic profiles.

We determined the optimal bacilli seeding densities for *Msm*, *Mtb* H37Rv and *Mtb* mc<sup>2</sup> 6230 by plotting the number of bacilli seeded against the basal OCR and ECAR levels (*Msm* seeding optimization shown in Figure 1). The optimal seeding number should be in the linear part of the bacilli number OCR/ECAR relationship. For *Msm* this was determined to be  $0.25 \times 10^6$  bacilli/well, and  $2 \times 10^6$  for both *Mtb* H37Rv and *Mtb* mc<sup>2</sup> 6230 (data not shown).

iii) The optimal concentration of the different inhibitors to achieve maximal responses will be determined by titration of each inhibitor with each mycobacterial species. We will use proprietary XF software specifically designed to analyze the data obtained from these experiments. We understand that characterization of these initial parameters holds key to all further experiments. We expect to accomplish the aims of subtask 1a by the end of 8 months.

We next determined the bioenergetic profile of *Msm* generated by careful titration some of the known electron transport chain (ETC) disrupters/inhibitors (Figure 2). Due to the short doubling time of *Msm* compared to that of *Mtb* H37Rv the data was continuously plagued by error due to bacilli dividing during the course of the experiment. We therefore proceeded with bioenergetic studies using different *Mtb* strains and did not continue the bioenergetic characterization of *Msm*.

For various *Mtb* strains we investigated effect of different ETC-targeting antimycobacterial drugs on *Mtb* bioenergetics. We focused on Clofazimine (CFZ, targets Complex I), Bedaquiline (BDQ/TMC207, targets Complex V) and Q203 (targets Complex III). Firstly we investigated the effect of CFZ and BDQ on the OCR profiles of *Mtb* mc<sup>2</sup> 6230 (Figure 3). These experiments were done in DMEM media with different concentrations of CFZ and BDQ (as indicated), and a CCCP concentration of 10  $\mu$ M. With CFZ we obtained an expected result – in all cases the OCR was raised to the same level due to uncoupling with CCCP, after which OCR decreased in a concentration dependent manner by the addition with of CFZ. The decrease in OCR is consistent with ETC complex inhibition. BDQ caused a very surprising concentration-dependent increase in OCR and not the expected decrease in OCR from a Complex V (ATP synthase) inhibitor. This increase in OCR after the addition of the BDQ suggests a more complex mechanism of action. Also, from these experiments we have proven that the XF96 can be optimized to study and/or screen for compounds that target the mycobacterial ETC complexes.

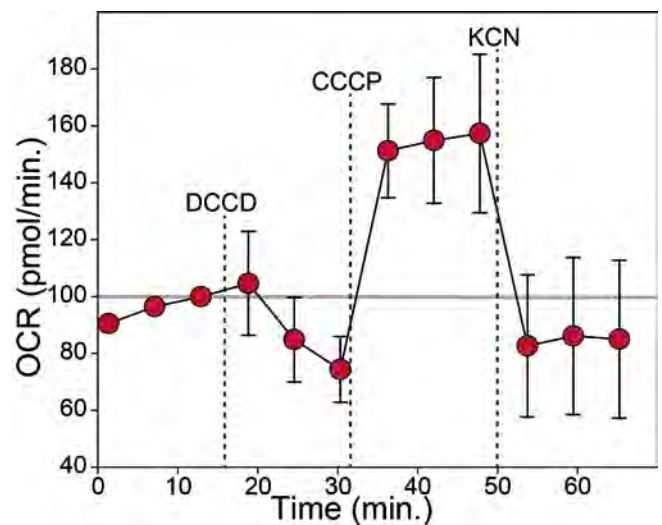


Figure 2: The complete bioenergetic profile of *Msm*. The dotted lines indicate the time points at which the different ETC disruptors/inhibitors were added - 25 $\mu$ M DCCD (ATP synthase inhibitor), 10 $\mu$ M CCCP (ETC uncoupler) and 100 $\mu$ M KCN (Cytochrome C oxidase inhibitor).

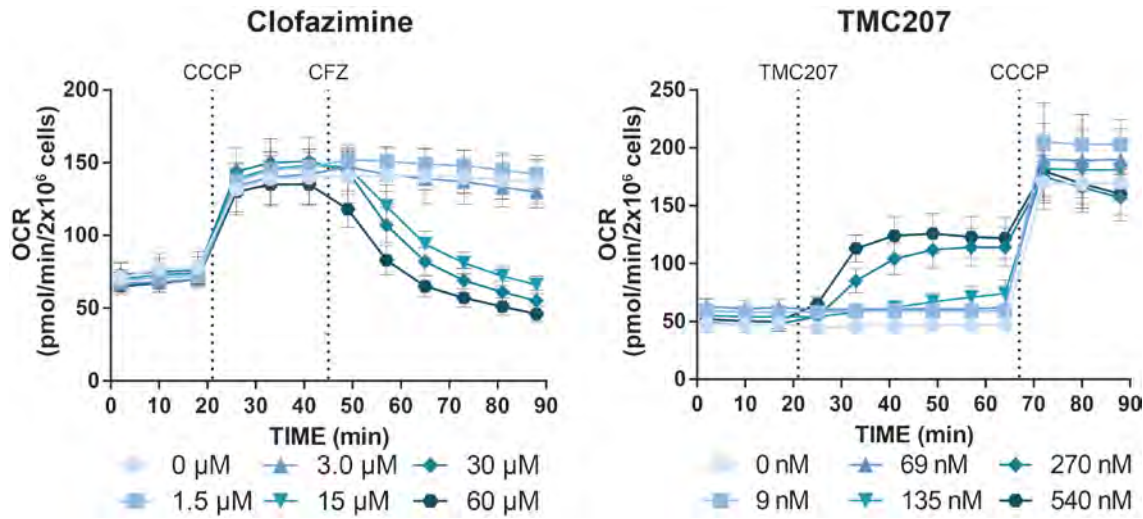


Figure 3: The initial OCR experiments done using the known anti-mycobacterial drugs CFZ and BDQ (TMC207), and *Mtb* mc<sup>2</sup> 6230. The dotted lines indicate the time points at which CFZ, BDQ and CCCP were added.

We next investigated whether different carbon sources would change the increase in OCR caused by BDQ, as well as the effect Q203 would have on mycobacterial bioenergetics. We also looked that the effect these drug have on mycobacterial ECAR in the presence of the different carbon sources. These experiments were done with *Mtb* H37Rv in modified 7H9 media. For this the bacilli were starved for 24 hrs prior to the start of the experiment in 7H9 media containing no carbon source. During the experiment a carbon source (glucose, lactate or palmitate) was added after three basal measurements were taking. After carbon source addition BDQ and Q203 were added respectively, followed by 2  $\mu$ M CCCP as indicated by the dotted lines in Figures 4 and 5.

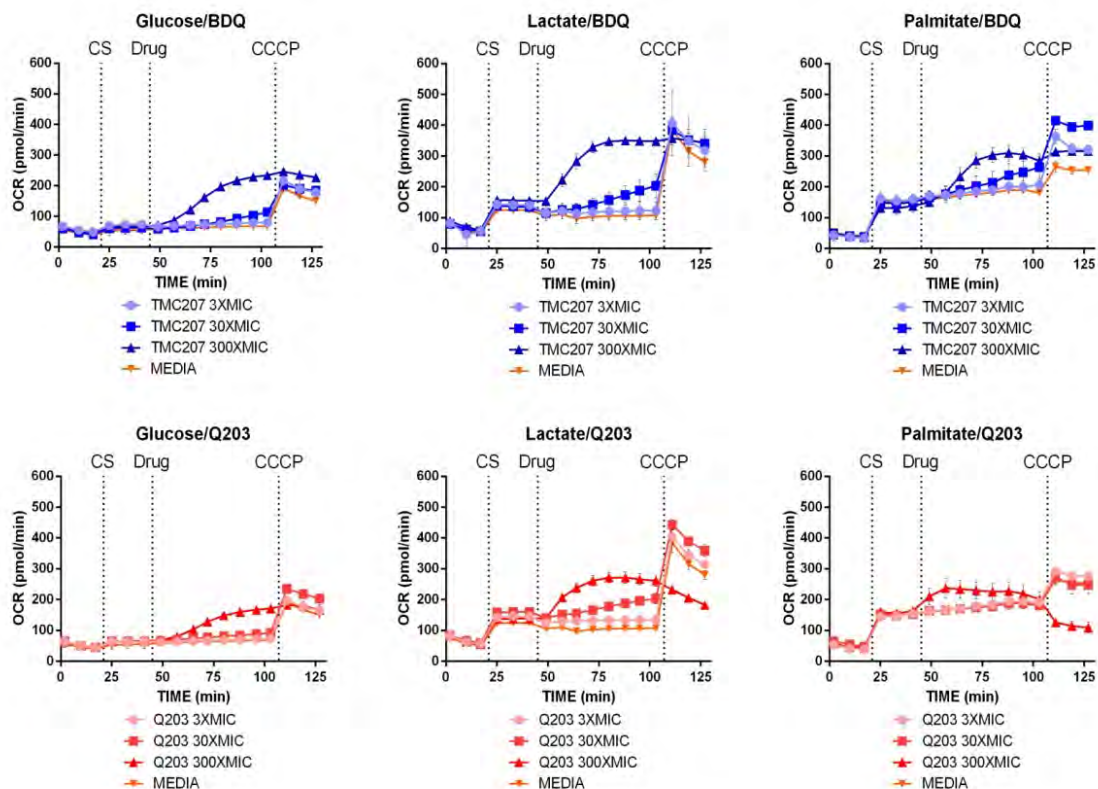
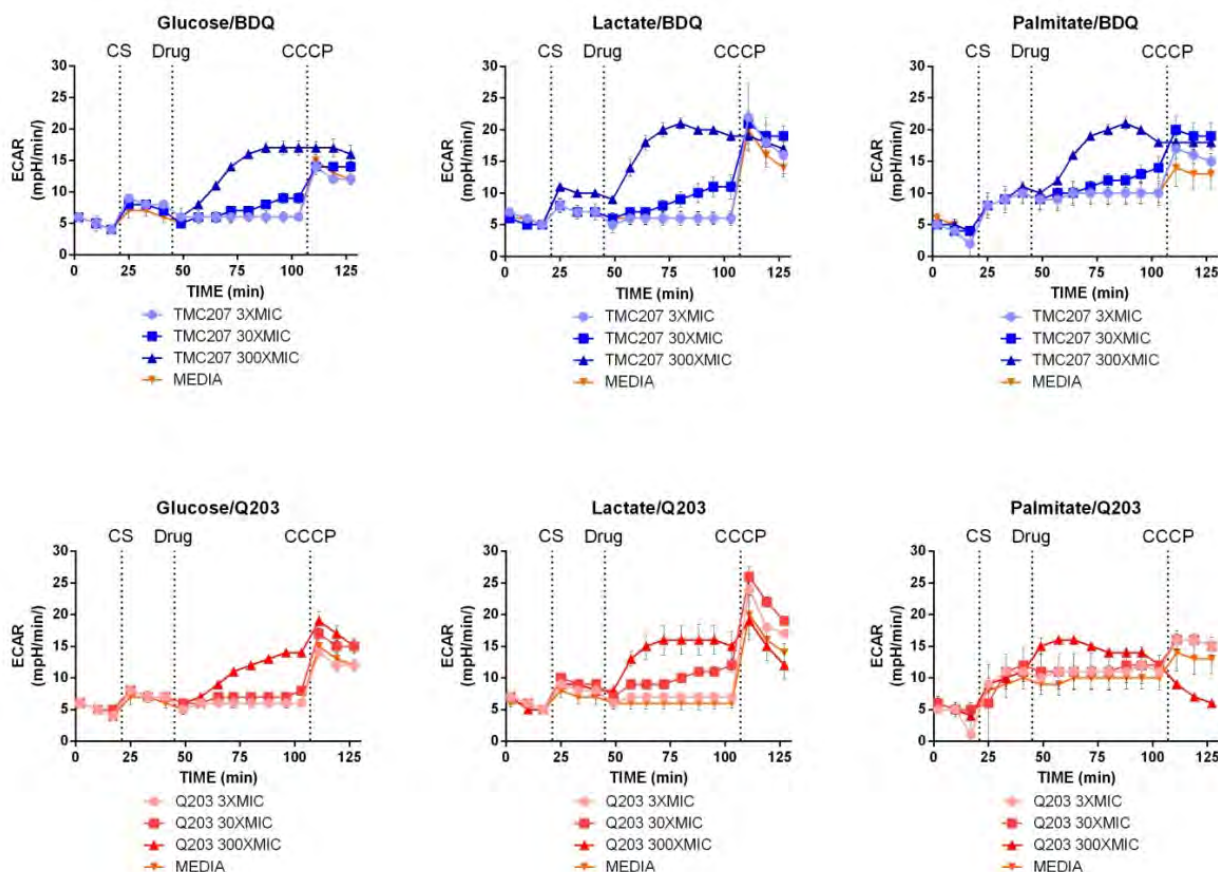


Figure 4: The OCR profiles of *Mtb* H37Rv. The dotted lines indicate the time points at which the different carbon sources, drug and CCCP were added. BDQ and Q203 have different effect on the OCR of mycobacteria in the presence of the carbon sources tested.



**Figure 5: The ECAR profiles of *Mtb* H37Rv.** The dotted lines indicate the time points at which the different carbon sources, drug and CCCP were added. BDQ and Q203 have different effect on the ECAR of mycobacteria in the presence of the carbon sources tested.

Firstly, Q203 (a Complex III inhibitor) also causes an increase in OCR – *also an unexpected result*. Also, both BDQ and Q203 cause an increase in ECAR which means that mycobacterial glycolysis is also stimulated upon addition. The stimulation of glycolysis would be to compensate for the lack of ATP production through OXPHOS and thus more ATP would be produced through glycolysis. It is also clear from the data that carbon source (glucose, lactate and palmitate) play a role in the bacilli's ability to maintain its membrane potential after drug addition. This has important implications for drug discovery seeing that mycobacterial carbon sources vary greatly from *in vitro* culturing and screening conditions, to *in vivo* infection conditions.

To establish the duration of increased OCR (from basal levels), we treated different *Mtb* H37Rv cultures with BDQ and Q203, at 30x and 300x their MIC concentrations. On specific days (0, 1, 3, 6 and 9) an aliquot was taken from these drug treated cultures and the basal respiration of the bacilli measured. The results (Figure 6) show that BDQ (at both concentrations) increases the basal respiration (as seen previously) when compared to an untreated control, after which basal respiration drops to almost zero at day 1 and zero at day 6 after drug treatment in the case of 300x MIC. The basal respiration of the bacilli treated with 30x MIC BDQ stays elevated for longer and does not reach zero for the 9 days the experiment continued. Both concentrations of Q203 show a slightly elevated basal OCR at day 0 and after that does not stray far from the basal respiration of the untreated media control. This shows that the inhibition of Complex V (ATP synthase) is more detrimental to mycobacterial OCR than the inhibition of Complex III (the cytochrome *bc<sub>1</sub>* complex), which can be explained by the expression of the cytochrome *bd<sub>1</sub>* complex compensating for the inhibition of Complex III.



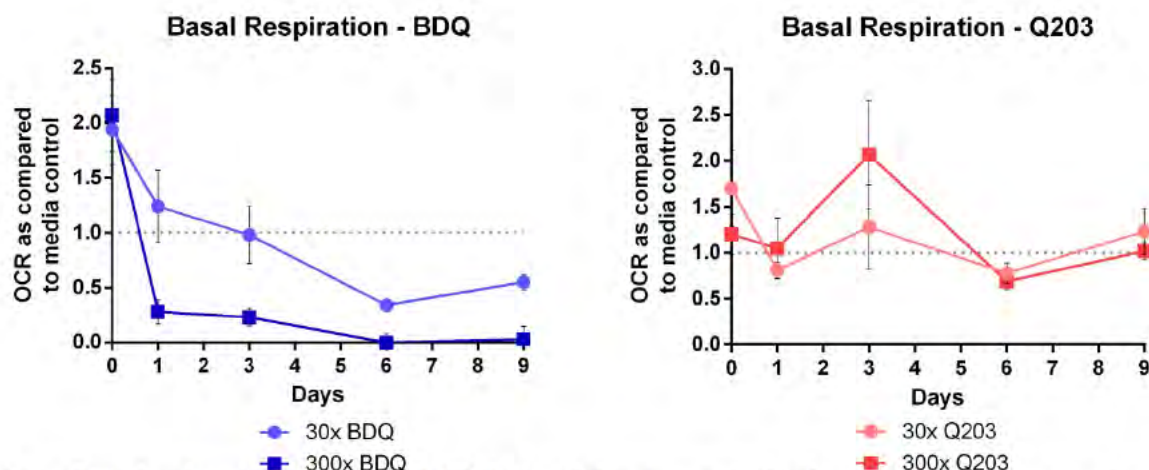


Figure 6: The basal respiration of BDQ and Q203 (at two different concentrations) treated cultures as compared to untreated cultures. BDQ has a more detrimental effect on mycobacterial OCR over nine days.

Finally, we used the XF96 in very unconventional way, the experiment was setup to allow for the probes of the XF96 sensor cartridge settle down and maintain the transient micro-chamber for four hours at a time. This allowed us to see how the OCR (here in mmHg/min) changes as a function of oxygen concentration (Figure 7). It is immediately clear from the data that in the presence of BDQ and Q203 the bacilli still have relatively high OCR's even in the presence of very low oxygen concentrations. The untreated bacilli's OCR reaches a near zero plateau at an oxygen concentration of ~100 mmHg, the same concentration found in the alveoli of the human lung. In contrast, the drug treated bacilli still have relatively high OCR at 100 mmHg and especially in the case of 300x MIC BDQ the bacilli still have a higher OCR at < 25 mmHg (borderline hypoxic) than the untreated bacilli had at 100 mmHg. Thus it seems that BDQ more so than Q203 have the ability to mess with the mycobacterial oxygen sensing mechanisms and force the bacilli to maintain high OCRs in near hypoxic oxygen concentrations. The ability to screen for compounds that force mycobacterial to consume oxygen will become very important in the development of compounds that target persistent/dormant mycobacteria and understanding the biology of latency.

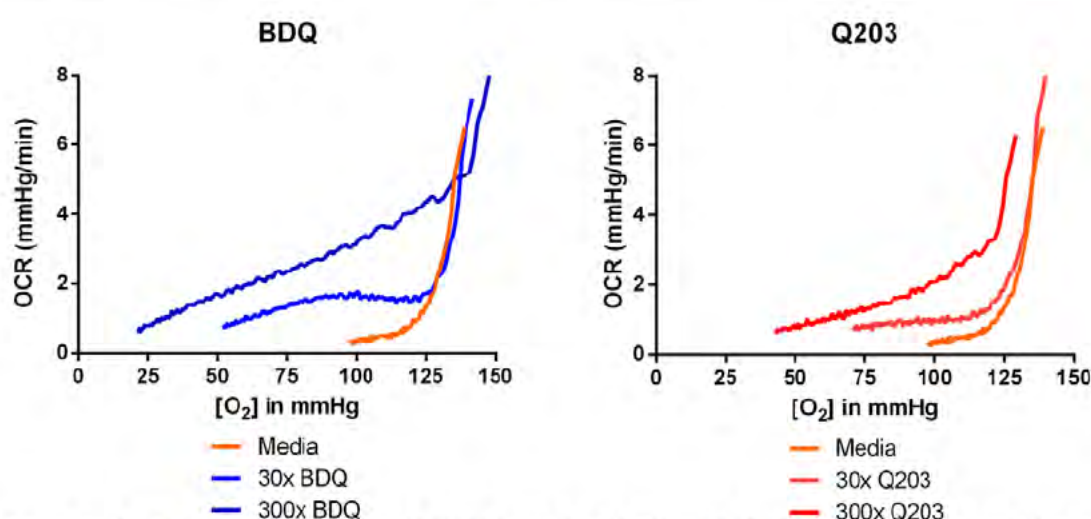


Figure 7: The OCR profiles of BDQ and Q203 treated, and untreated *Mtb* H37Rv as a function of oxygen concentration. Mycobacteria are forced to oxygen at much lower oxygen concentration when treated with BDQ and Q203, than when left untreated.



**Subtask 1b. (Months 9-12) To determine the bioenergetic profile of various mycobacterial genetic mutants ( $\Delta whiB3$ ,  $\Delta whiB4$ ,  $\Delta senX$ ,  $\Delta regX$ ,  $\Delta sigH$ ,  $\Delta mshA$  and  $\Delta dosR$ ) used in this study).** To characterize the bioenergetic profile of above mentioned mycobacterial mutants, we will follow the approach mentioned in subtask 1a and the cell density for each mutant will be determined. We will be guided by the data obtained from the results of experiments performed in subtask 1a and should be able to characterize the mutants by the end of 12 months.

We first accessed whether there is bioenergetic difference between *Mtb* H37Rv and *Mtb* H37Rv  $\Delta whiB3$ . In the first set of experiments both wild type and mutant bacilli were starved in 7H9 media containing no carbon source for 24 hrs prior to the start of the experiment. During the experiment three basal measurements were taken before the addition of the different carbon source combinations as indicated on Figure 8, after which CCCP was added (2  $\mu$ M). The increase in OCR after the addition of the different carbon source combinations is distinctly different in the wild type and mutant bacilli. Also, after uncoupling the wild type bacilli are able to maintain their membrane potential independent of carbon source whereas maintaining  $\Delta whiB3$  membrane potential seems more carbon source dependant. This shows that *Mtb* H37Rv and *Mtb* H37Rv  $\Delta whiB3$  utilize carbon sources differently and that WhiB3 may play a role in controlling carbon source utilization.

In a second set of experiments *Mtb* H37Rv and *Mtb* H37Rv  $\Delta whiB3$  bacilli were starved in PBS containing no carbon source for 2 and 4 weeks prior to the start of the experiment (Figure 9). Control bacilli were cultured in 7H9 containing OADC and glycerol. The experiment was done as described above. Firstly, after two and four weeks of starvation both wild type and mutant bacilli were still able to respond fairly quickly to the addition of carbon sources and CCCP. This again shows to the potential of using the XF96 to study mycobacterial metabolism and latency biology. Secondly, it seems that wild type bacilli have a more controlled and greater response to the addition of the carbon sources before and after the addition of CCCP when compared to the  $\Delta whiB3$  bacilli, which shows to WhiB3 playing some role in controlling carbon source sensing and utilization.

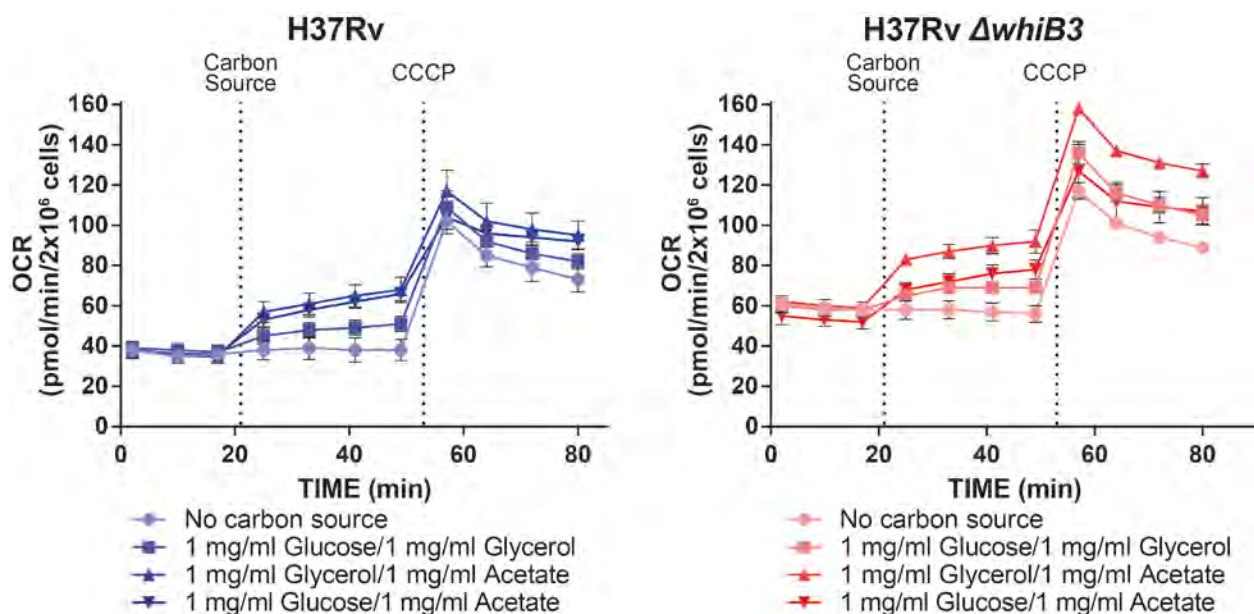


Figure 8: The OCR profiles of *Mtb* H37Rv and *Mtb* H37Rv  $\Delta whiB3$  in the presence of different carbon source combinations. The dotted lines indicate the time points at which the different carbon sources and CCCP were added.

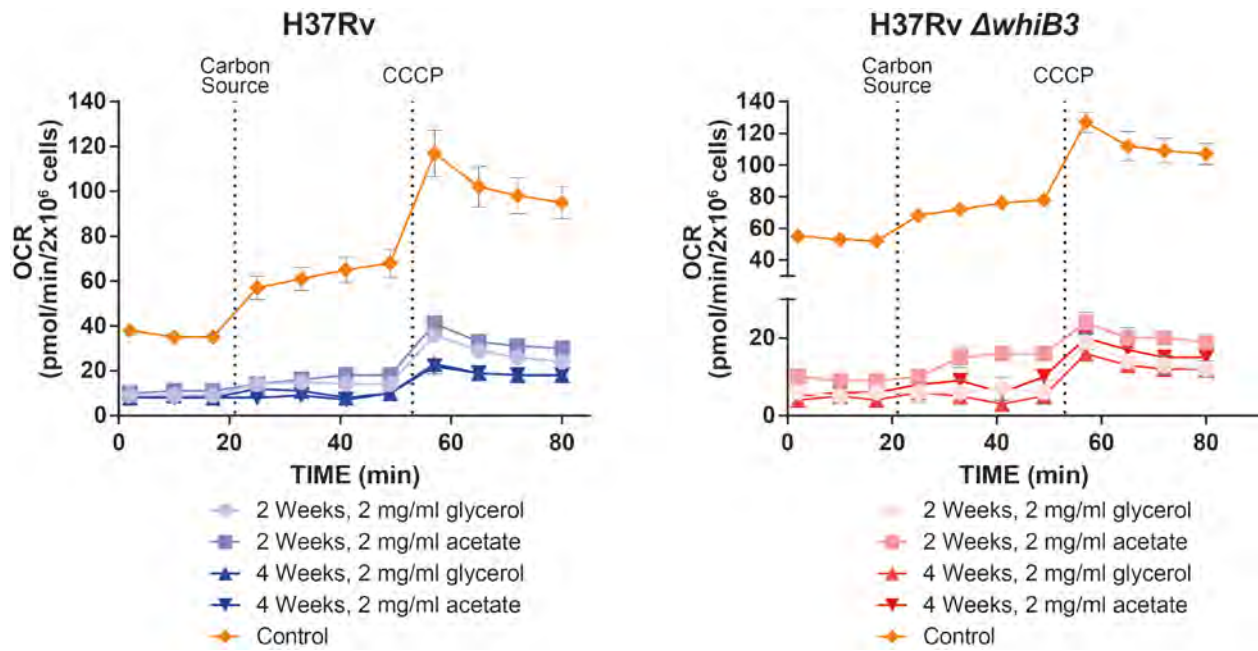


Figure 6: The OCR profiles of *Mtb* H37Rv and *Mtb* H37Rv  $\Delta$ whiB3, which were starved in PBS for two and four weeks, in the presence of different carbon source combinations. The dotted lines indicate the time points at which the different carbon sources and CCCP were added.

To determine the influence of WhiB3 on mycobacterial bioenergetics, metabolic flux of wt *Mtb*, *Mtb* $\Delta$ whiB3 and the complemented strain was examined by measuring their oxygen consumption rate (OCR, a measurement of oxidative phosphorylation) and extracellular acidification rate (ECAR, a measurement of glycolysis) using a XF96 Extracellular Flux Analyzer (Seahorse Biosciences, MA, USA) (Figure 10E, 10G). After basal metabolic flux was measured, an electron transport chain (ETC) uncoupler, carbonyl cyanide *m*-chlorophenyl hydrazone (CCCP), was added and we observed an increase in the OCR and ECAR in all three strains. Normalized basal OCR and ECAR measurements in Figure 10F and 10H indicate that after CCCP addition, OCR and ECAR of *Mtb* $\Delta$ whiB3 was significantly greater than that for wt *Mtb* and the complemented strain, respectively. This could be due to the depolarized membrane potential observed in *Mtb* $\Delta$ whiB3 (data not shown here), where *Mtb* $\Delta$ whiB3 attempts to increase the efflux of protons to a greater degree than the other two strains to prevent complete collapse of the already depolarized membrane potential. Figure 10I shows the oxidative:glycolytic ratio (OCR/ECAR) for the normalized data of the three strains prior to and after the addition of CCCP indicated by 1, 2 and 3 on Figures 10F and 10H. The OCR/ECAR value is an indication of the overall bioenergetic state of a cell, where OCR/ECAR < 1 indicates more glycolytic-dependent bioenergetics and OCR/ECAR > 1 indicates more OXPHOS-dependent bioenergetics. Four minutes after the addition of CCCP (2 on Figures 10F, 10H), metabolism shifted towards glycolysis (OCR/ECAR < 1) in all three strains, with *Mtb* $\Delta$ whiB3 being significantly more glycolytic than wt *Mtb* and the complemented strain. There were no significant differences in OCR/ECAR between wt and complemented strains. Thirty minutes after CCCP injection (3 on Figures 10F, 10H), wt *Mtb* and the complemented strains were able to shift their energy metabolism back to equilibrium, OCR/ECAR  $\approx$  1, whereas *Mtb* $\Delta$ whiB3 was only able to reach OCR/ECAR of  $\approx$ 0.7.

The phenogram in Figure 10J of the fourth measurement 30 minutes after CCCP addition also demonstrates that *MtbΔwhiB3* is more glycolytic than wt *Mtb* and complemented strains. Taken together, metabolic flux analyses conclusively demonstrate the inability of the *MtbΔwhiB3* to control and maintain bioenergetic homeostasis.

Respiration implicates energy metabolism in the synchronization of lipid metabolism. This is supported by our bioenergetic data, which point to a critical role for energy balance in polyketide and lipid synthesis under *WhiB3* control. We adapted a novel technology termed metabolic flux analysis and demonstrated that *MtbΔwhiB3*, unlike wt *Mtb* and the complemented strain, was unable to re-establish bioenergetic homeostasis between glycolysis and OXPHOS after uncoupling the energized membrane (Figures 10E-J).

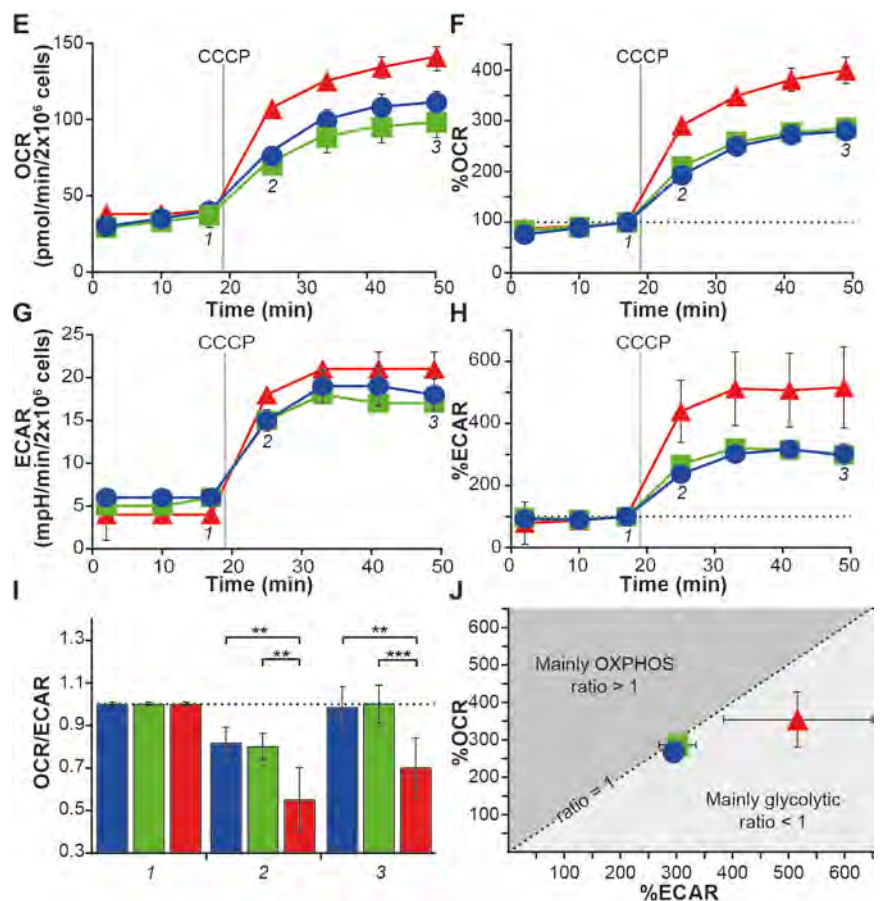


Figure 10: The influence of *WhiB3* on mycobacterial bioenergetics.

We have also recently started to investigate the link between mycobacterial metabolism and redox homeostasis using the XF96. For these experiments we are going to use bacilli deficient in either one of the two small molecule thiols associated with redox homeostasis in mycobacteria, mycothiol (MSH) and ergothionine (ERG). The ERG deficient mutants are *Mtb* CDC1551  $\Delta$ *egtA* and *Mtb* CDC1551  $\Delta$ *egtD*, and the MSH deficient mutant is *Mtb* CDC1551  $\Delta$ *mshA*. The OCR profiles of the  $\Delta$ *egtA* strain, along with its wild type and complimentary strains, and four different carbon sources are shown in Figure 11. The data shows that there is no difference in the ability of  $\Delta$ *egtA* to maintain its membrane potential in the no carbon source (media) control, as well as when cholesterol is used as a carbon source. In the presence of the other carbon sources (glucose, acetate and palmitate) tested there are varying degrees of difference between  $\Delta$ *egtA* and the wild type strain to maintain their membrane potential. This shows towards a link between ERG mediated redox homeostasis and the catabolism of carbon sources that directly feed into the TCA cycle, although further evidence is needed to prove this conclusively.



4.

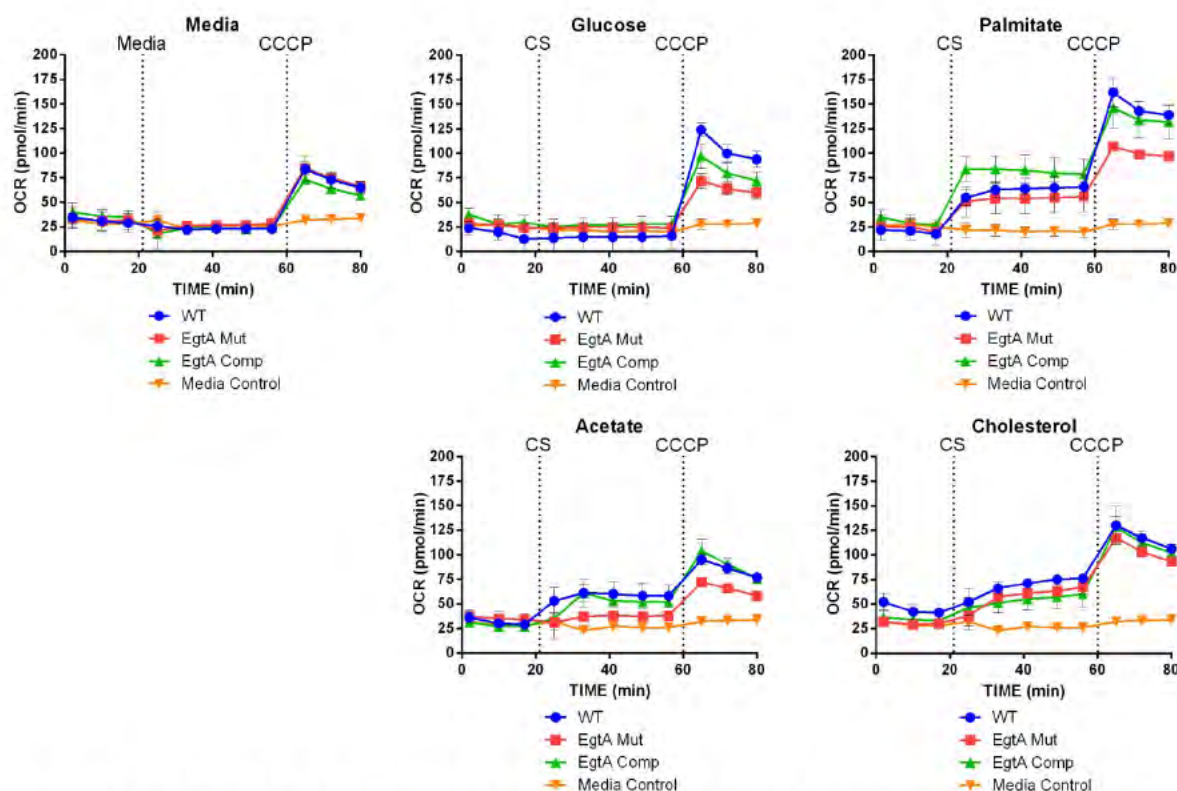


Figure 11: The OCR profiles of *Mtb* CDC1551 and *Mtb* CDC1551  $\Delta$ *egtA* (and its' complemented strain) in the presence of different carbon source combinations. The dotted lines indicate the time points at which the different carbon sources and CCCP were added. This data establishes a link between ergothioneine mediated redox homeostasis and metabolism.

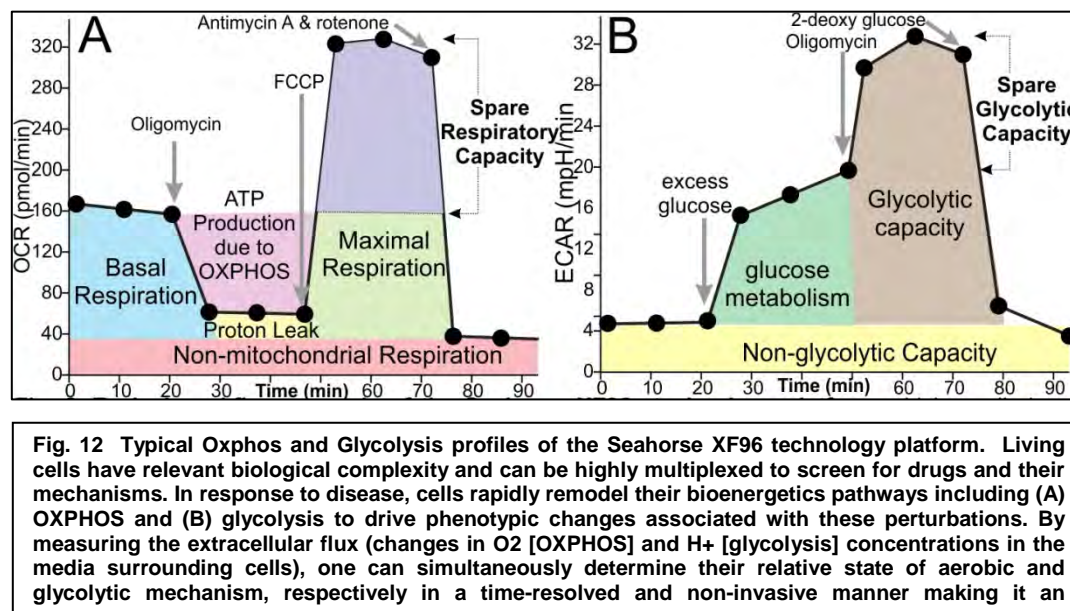
**TASK 2. (Months 13-18)** To determine the bioenergetic profile of human cells and to examine the effect of *Mtb* infection and mutants thereof on host bioenergetics.

**Subtask 2a. (Months 13-14)** To characterize of the bioenergetic profile of THP-1 cells. Once the characterization of mycobacterial species and their mutants is accomplished, as a component of our specific aim 2, we will focus on defining the bioenergetic profile of human monocyte THP-1 cells. These cells will be differentiated into adherent, well-spread macrophages by the addition of 10 ng/ml phorbol myristate acetate (PMA). Viability of THP-1 cells to ascertain appropriate seeding density will be determined via trypan blue exclusion assay. The bioenergetic profile will be determined using similar approaches as used for subtasks 1a and 1b. Non-buffered media will be used to determine the bioenergetics profile of the cells in the XF96 flux analyzer.

While our original approach for TASK 2 was to use the human monocyte cell line (THP-1), we instead began our bioenergetics profiling of mammalian cells using RAW264.7 mouse macrophages due to their increased relevance to our animal model of *Mtb* infection. This cell line is adherent and allows known cell numbers to be seeded into the XF cell culture plate for rapid optimization. Initially, the technology for the extracellular flux analysis of *Mtb*-macrophage interaction was optimized. We first determined the optimal cell density of macrophages that forms a uniform monolayer of cells at the base of the well to ensure reproducible measurements of OCR and ECAR between wells and plates. In the OXPHOS profile (Fig. 12A), the mean basal respiration is determined by taking 3-4 OCR measurements before the addition of the inhibitors or activators.

ATP-linked OCR and proton leak were determined by injecting oligomycin A. The reduction in OCR following oligomycin A injection is the rate of oxygen consumption that corresponds to ATP synthesis, and the oligomycin-insensitive OCR rate is considered as  $H^+$  leak across the mitochondrial membrane. FCCP, an uncoupler of the ETC was used to determine the maximal

respiration, which gives the theoretical maximum oxygen consumption that can take place at the cytochrome c oxidase whether limited by availability of substrate or activity of the ETC. The difference between the basal OCR and the FCCP stimulated OCR is the spare respiratory capacity (SRC) of the cell, which is a measure of the extra capacity of the cell available to utilize under conditions of stress and/or increased energetic demands. Antimycin A, an inhibitor of complex III, and rotenone, an inhibitor of complex I were used to completely inhibit mitochondrial electron transport. The OCR determined after the injection of antimycin A and rotenone is attributable to non-mitochondrial O<sub>2</sub> consumption. At the end of each assay, OCR and ECAR values can be



normalized to the protein content or cell number in each well. The concentrations of these mitochondrial modulators were optimised on the RAW264.7 macrophages in order to measure these bioenergetic parameters. Refer to the OXPHOS (OCR) profiles of the non-infected RAW264.7 cells in Fig 13.

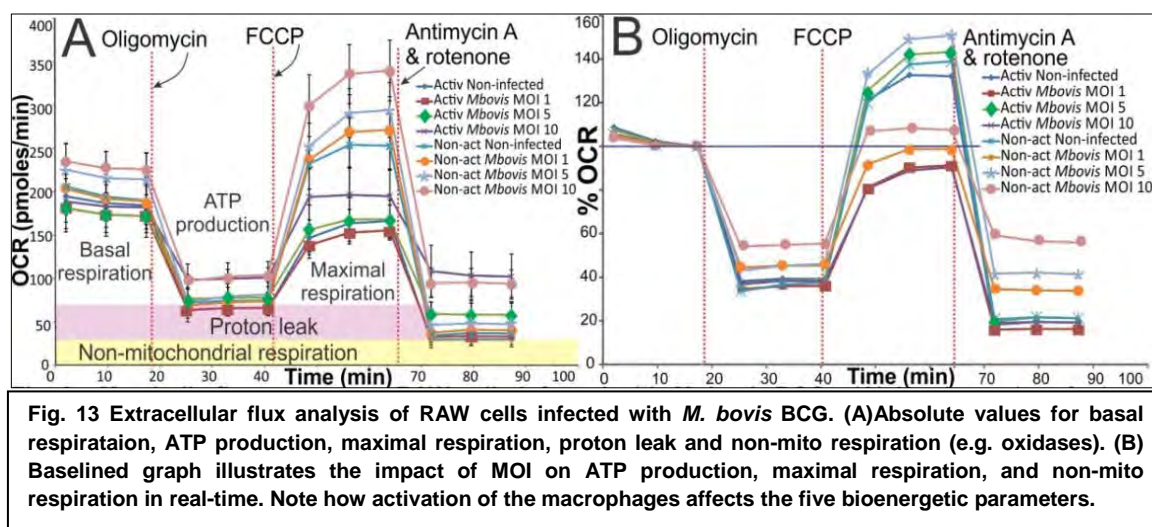
In the glycolytic profile (Fig. 12B), basal ECAR due to lactate is initially measured by 3-4 ECAR measurements in XF medium without glucose. After the addition of glucose, the ECAR due to glycolysis is determined. Oligomycin is then injected to inhibit ATP synthase in the ETC, which induces maximal glycolysis to provide the ATP requirements of the cell. The difference in ECAR between the maximal glycolysis and the glycolysis induced by the addition of glucose gives a measure of the glycolytic reserve. An inhibitor of hexokinase, 2-deoxyglucose, is injected to inhibit glycolysis to verify that the increase in ECAR is due to glycolysis. The protocol on the XF and concentration of oligomycin were optimized for RAW264.7 cells. Refer to glycolytic (ECAR) profiles of the non-infected RAW264.7 cells in Fig. 15.

**Subtask 2b. (Months 15-18) To examine the effect of Mtb infection and mutants thereof on host bioenergetics.** To investigate the effects of Mtb infection and the mutants thereof on host cells, we will infect differentiated THP-1 cells at a low MOI (1:1). Briefly, THP-1 cells, at an appropriate seeding density, will be infected with different mycobacterial strains. After 4 hr of infection, cells will be washed (twice) with PBS supplemented with gentamycin (100ug/ml) to kill any extracellular bacteria. This will be followed by a PBS-only wash to remove traces of gentamycin. Non-buffered media will be used to determine the bioenergetic profile of these infected cells in the XF96 flux analyzer.



Next, optimization of bioenergetic profiling of mycobacterium-infected RAW264.7 macrophages was achieved using a non-pathogenic strain of mycobacteria, *M. bovis* BCG, due to the added difficulties of working in a BSL3 environment. Once the profiling of non-pathogenic mycobacterial infections was established, the XF96 was moved into a BSL3 facility.

RAW264.7 mouse macrophages (both resting and activated) were infected with *M. bovis* BCG at a multiplicity of infection (MOI) of 1, 5, and 10. OXPHOS profiles were generated daily over a 5 day infection. Fig. 13 demonstrates how the MOI of *M. bovis* BCG impacts the bioenergetic parameters of the infected host cell. An infection of MOI of 1 and 5 increased the basal respiration of resting macrophages (Fig 13A). The baselined profile in Fig 13B shows that an increase in MOI decreases the ATP turnover and increases the proton leak after oligomycin A injection. Addition of FCCP



(an ETC uncoupler) indicates that infection substantially reduces the maximal respiration and SRC of the infected macrophages. This indicates that the cell has little reserve for increased energy demands or stressful environments. Conversely, non-mitochondrial respiration is increased in these infected cells, possibly due to the production of reactive oxygen species.

Of note, infection of macrophages with *M. bovis* BCG over a five day period shows that macrophage bioenergetics metabolism has shifted from contributions from both OXPHOS (OCR) and Glycolysis (ECAR) on day 1 to much reduced OXPHOS and increased ECAR on day 5 of the infection (Fig. 14).

We next tested how the MOI of *Mtb* infection impacts the bioenergetic parameters (ECAR and OCR) of RAW264.7 macrophages. An MOI of 10 has deleterious effects on both OXPHOS and glycolysis of macrophages after 96 hrs, while an MOI of 5 appears to stabilize glycolysis of infected RAW cells (Fig. 15). In the OCR experiments, at 6 hours, *Mtb* infection decreased OXPHOS ATP turnover and possibly redirected bioenergetic metabolism to glycolysis. By using the OCR, ECAR and the combination of inhibitors as described above in a single microplate, it becomes possible to pinpoint sites of action of drugs on macrophage ETC function. These data reveal an important novel finding, which is that a particular MOI may stabilize bioenergetic pathways in the host cell in order to maintain the host's viability to perpetuate survival of the bacillus.

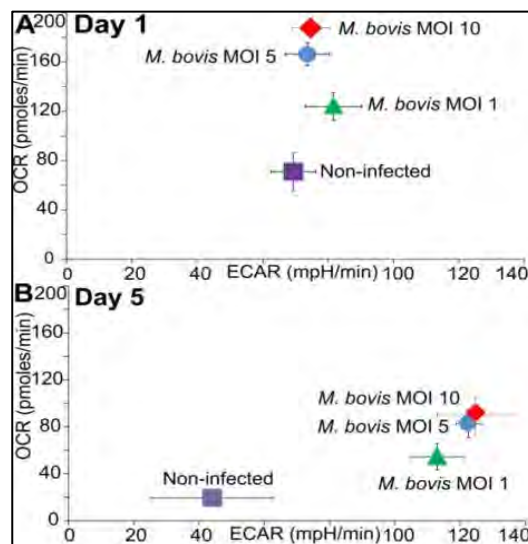
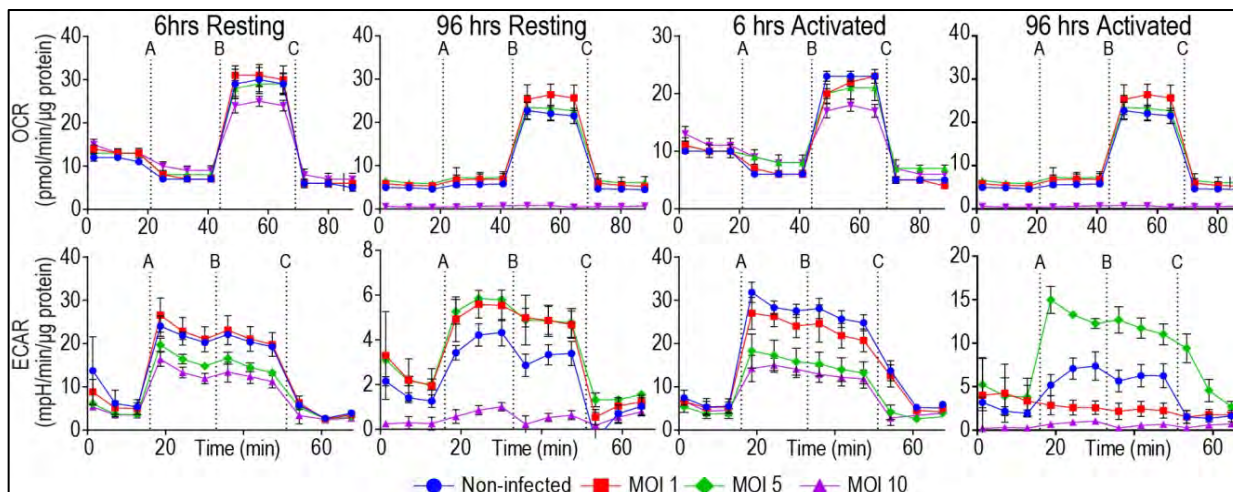


Fig. 14. Plot of OCR vs ECAR for *M. bovis* BCG infection of RAW cells on (A) Day 1 and (B) Day 5. The plots indicate a shift from OXPHOS (indicated by OCR) in the *M. bovis* BCG-infected RAW on Day 1 to glycolysis (indicated by ECAR) on Day 5 of the infection.





**Fig. 15. MOI of *Mtb* infection affects the OXPHOS (Top panel) and Glycolytic (Bottom Panel) bioenergetic profiles of resting and activated RAW264.7 cells after 6 and 96 h of infection. Metabolic modulators injected at the time points indicated by the vertical dotted lines include: (A) Oligomycin, (B) FCCP, (C) antimycin A and rotenone in the OXPHOS bioenergetic profiles (Top Panel) and (A) Glucose, (B) Oligomycin and (C) 2-deoxyglucose in the glycolytic bioenergetic profiles (Bottom Panel). Note the deleterious effects of an MOI of 10 on host metabolism, whereas an MOI of 5 appears to**

OXPHOS profiles of human monocytes isolated from peripheral blood mononuclear cells and infected with *Mtb* at varying MOIs are demonstrated in Fig. 16. *Mtb* infection of human monocytes decreased the ATP-linked OCR of monocytes with increasing MOI, increased maximal respiration and SRC and increased monocyte non-mitochondrial respiration. The large non-mitochondrial respiration observed at an MOI of 5 indicates that the maximal respiration observed after FCCP addition is not due to oxygen consumption in the electron transport chain. The OXPHOS profiles of monocytes isolated from a healthy volunteer and a TB patient (not yet on drug therapy) were also determined using XF96 technology (Fig. 16, right panels). The SRC of peripheral blood monocytes in a TB patient was substantially reduced. Note that both OCR and ECAR are measured simultaneously and are an effective indicator of compounds that either shift or restore host metabolism.

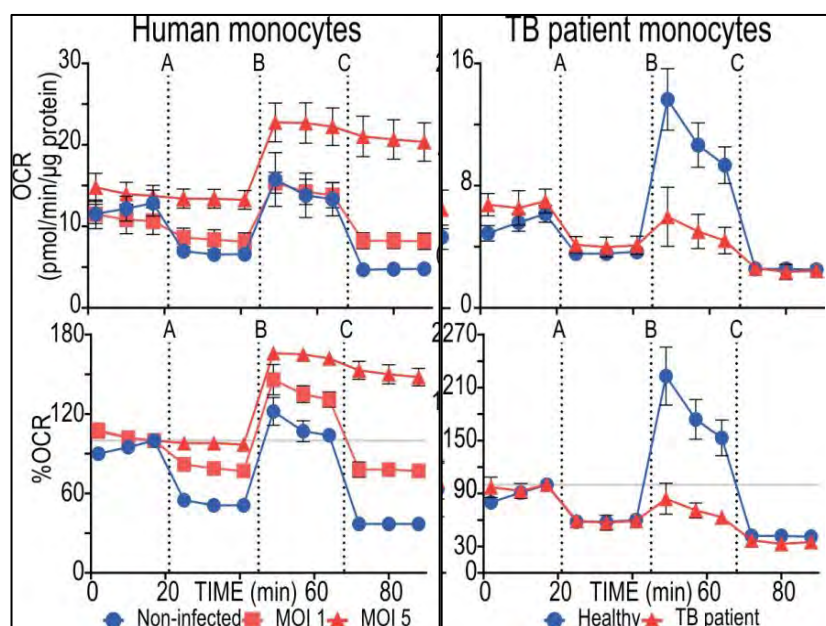


**Fig. 16. *Mtb* infection alters the OXPHOS bioenergetic profiles of human monocytes isolated from PBMC, and monocytes isolated from PBMC of a TB patient and healthy control have different OXPHOS profiles. Mitochondrial modulators injected at the time points indicated by the vertical dotted lines include: (A) Oligomycin, (B) FCCP, (C) antimycin A and rotenone. Profiles baselined at basal respiration (grey horizontal line) are displayed below each profile to demonstrate differences in ATP-linked OCR, maximal respiration and non-mitochondrial respiration. Note the dramatically reduced SRC of the TB patient blood monocytes in comparison to that of the healthy control. Infection of human monocytes with an MOI of 5 decreases the ATP-linked OCR and substantially increases maximal respiration and non-mitochondrial respiration of the monocytes.**

## KEY RESEARCH ACCOMPLISHMENTS:

- We have successfully adapted metabolic flux analysis using a Seahorse XF96 metabolic flux analyzer to study *Mycobacterium tuberculosis* energy metabolism in an unparalleled way. *Using this novel method, for the first time, we non-invasively measured the metabolic activity of intact bacilli, thereby providing novel data on basal O<sub>2</sub> consumption rates (OCR), glycolysis rates (extracellular acidification rates; ECAR), ATP turnover and reserve respiratory capacity in a single experiment.*
- We have examined a range of *Mtb* mutants and have characterized the role of several genes in *Mtb* energy and redox homeostasis.
- Using flux analysis, we made several novel discoveries, including, but not limited to determining that the new antimycobacterial drug Bedaquiline (BDQ), and Q203 (a new phase I drug) dramatically increases *Mtb* respiration in a concentration dependent manner. *This suggests that the accepted modes of action of these anti-TB drugs are far more complex than previously thought.*
- Contrary to the mode of action of BDQ and Q203, CFZ's mode of action was distinctly different.
- Metabolic flux analyses conclusively demonstrate that *Mtb* WhiB3 is required for control and maintenance of bioenergetic and metabolic homeostasis.
- Metabolic flux analyses of the *Mtb* *egt* mutants established a clear link between intracellular redox balance and energy metabolism.
- Metabolic flux analyses of murine RAW264.7 cells infected with *M. bovis* BCG mycobacterium show a shift in host cell metabolism away from OXPHOS and towards glycolysis.
- Infection of murine RAW264.7 cells with *Mtb* suggests that certain MOI may actually stabilize bioenergetics pathways to maintain survival of the bacillus in the host.
- Monocytes from *Mtb*-infected humans show markedly decreased spare respiratory capacity compared with uninfected control subjects.
- Our findings establish a new paradigm of microbial energy metabolism in microbial pathogenesis and is anticipated to have broad impact.

**5. CONCLUSION:** *Mtb* persistence, as well as the known limitations of current anti-TB drugs and their inability to act on dormant bacilli, underscore the need to use innovative tools to examine the bioenergetic mechanisms that allow *Mtb* to enter, maintain and emerge from a persistent state of infection. We have successfully adapted a cutting-edge technology toward yielding a detailed understanding of *Mtb* bioenergetics, and its role in the mode of action of antimycobacterial drugs. Characterization of a genetically intractable and global pathogen such as *Mtb* is significant because it is the first step toward identifying bioenergetic pathways and components that modulate these pathways and could lead to strategies that will allow persistent and drug-resistant *Mtb* to be pharmacologically controlled. In addition, our findings will not only be applicable to the

prevention/treatment of other human pathogens, but will also contribute to a broader understanding of how microbial and infected host bioenergetics can be modulated as an approach to therapy.

## 6. PUBLICATIONS, ABSTRACTS AND PRESENTATIONS:

### a. manuscripts and abstracts

#### *Book Chapters:*

1. Steyn AJC, Mai D, Saini V and Farhana A. Protein-protein interaction in the -omics era: ***Understanding Mycobacterium tuberculosis function***. In: *Systems Biology of Tuberculosis*. Editors: J McFadden, D Beste and A Kierzek. 2013. Springer, New York, NY.
2. Cumming B, Lamprecht D, Wells R, Saini V, and Mazorodze J, and Steyn AJC. ***The Physiology and Genetics of Oxidative Stress in Mycobacteria***. In: *Molecular Genetics of Mycobacteria*. Editors: Graham F Hatfull and William R Jacobs Jr. 2nd Edition, 2014. ASM Press, Washington, DC

#### *Published:*

1. ***S100A8/A9 proteins mediate neutrophilic inflammation and lung pathology during tuberculosis***. Gopal, R; Monin, L; Torres, D; Slight, S; Mehra, S; McKenna, K; Junecko, B; Reinhart, T; Kolls, J; Baez-Saldana, R; Cruz-Lagunas, A; Rodriguez-Reyna, T; Kumar, N; Tessier, P; Roth, J; Selman, M; Becerril-Villanueva, E; Baquera-Heredia, J; Cumming, B; Kasprowicz, V; Steyn, AJC; Babu, S; Kaushal, D; Zuniga, J; Vogl, T; Rangel-Moreno, Jr; Khader, S. *American Journal of Respiratory and Critical Care Medicine*, 2013. 188(9):1137-46.

#### *Submitted or under review*

1. ***Mycobacterium tuberculosis WhiB3 is a global metabolic regulator that modulates the host cell-cycle.*** Bridgette M. Cumming, Dirk A. Lamprecht, Aisha Farhana, Kyle H. Rohde, Vikram Saini, Amit Singh, David G. Russell and Adrie J.C. Steyn. 2015. ***Cell Reports (CELL-REPORTS-D-14-02139)***
2. ***Untargeted metabolomic discovery of a redox hierarchy in mycobacteria and human tuberculosis.*** Vikram Saini, Bridgette M. Cumming, Loni Guidry, Dirk Lamprecht, John H. Adamson, Vineel Reddy, Krishna C. Chinta, Joel N. Glasgow, Anaximandro Gomez-Velasco, Yossef Av-Gay, Horacio Bach, Victoria Kasprowicz, Mandhir Munasur, Chih-Yuan Chen, Rajhmun Madansein, Jacques H. Grosset, Deepak Almeida, Hyungjin Eoh, Kyu Rhee and Adrie J.C. Steyn. 2015 ***Cell Host & Microbe (CELL-HOST-MICROBE-D-13-00506)***.
3. ***Heme oxygenase-1 protects against human tuberculosis by modulating inflammatory cells.*** Krishna C. Chinta, Vikram Saini, Joel N. Glasgow, Gene P. Siegal, Rajhmun Madansein, Gerard R. Alexander, Ryan M. Wells, Shepherd Nhamoyebonde, Alasdair Leslie, Veena B. Antony, Jessy Deshane, Anupam Agarwal and Adrie J.C. Steyn. 2015. ***Journal of Clinical Investigation (Ref# 79973-BR-1)***.



4. **Heme Oxygenase-1 Contributes To Host Defense In Non Tuberculous Mycobacterial Infections In Aging.** Ranu Surolia, Suman Karki, Zheng Wang; Hitesh Batra, Fu Jun Li, Tejaswini Kulkarni, Victor J Thannickal, Adrie JC Steyn, Anupam Agarwal, Veena B Antony. *The FASEB Journal* (Ref# FASEBJ/2014/267658).

*In preparation*

1. **Bedaquiline, Q203, and Clofazimine: Novel insights into effects on *M. tuberculosis* respiration.** Dirk A. Lamprecht, Peter M. Finin, Bridgette M. Cumming, Aejaz Rahman and Adrie J.C. Steyn. *To be submitted in 2015.*

#### **b. presentations during reporting period**

##### *Poster Presentations*

1. **4<sup>th</sup> SA TB Conference, 10-13 June 2014, Durban, South Africa. A novel anti-mycobacterial drug screen using real time measurements of mycobacterial bioenergetics.** Dirk A. Lamprecht, Bridgette M. Cumming and Adrie J.C. Steyn.
2. **Keystone Symposium: Novel Therapeutic Approaches to Tuberculosis.** Keystone, Colorado. March 30—April 4, 2014. **Skewing of host bioenergetic metabolism from oxidative phosphorylation to glycolysis: potential TB therapeutic approach.** Bridgette M Cumming, Adrie JC Steyn.
3. **Keystone Symposia Conference: Host Response in Tuberculosis.** 22-27 January 2015, Santa Fe, NM, USA. **Bedaquiline, Q203, and Clofazimine: Novel insights into effects on *M. tuberculosis* respiration.** Dirk A. Lamprecht, Peter M. Finin, Bridgette M. Cumming, Aejaz Rahman and Adrie J.C. Steyn.

##### *Oral Presentations*

1. **Seventh Annual New England Tuberculosis Symposium: The Convergence of the Infectious and Metabolic Diseases.** Boston, MA, October 9, 2013. **Redirecting host energy metabolism by *Mycobacterium tuberculosis*.** Adrie JC Steyn.
2. **South African H3-D Symposium.** Hermanus, South Africa, November 2013. **Screening for drugs that redirect energy metabolism: A new paradigm for antimycobacterial drug discovery?** Adrie JC Steyn.
3. **5<sup>th</sup> Southeastern Mycobacteria Meeting.** Birmingham, Alabama. January 24-26, 2014. **Energy and redox homeostasis during *Mycobacterium tuberculosis* infection.** Adrie JC Steyn.
4. **Keystone Symposium: Novel Therapeutic Approaches to Tuberculosis.** Keystone, Colorado. March 30—April 4, 2014. **Untargeted Metabolomic Discovery of a Redox Hierarchy in *Mycobacteria* and Human Tuberculosis.** Adrie JC Steyn.
5. **9<sup>th</sup> International Conference on the Pathogenesis of Mycobacterial Infections.** June 26-29, 2014. Saltsjöbaden, Sweden. **Metabolomic discovery of a redox and bioenergetic hierarchy in *M. tuberculosis* and in human TB.** Adrie JC Steyn.
6. **Nelson Mandela School of Medicine College Symposium 2014, 11-12 September 2014, Durban, South Africa.** **Real time mycobacterial bioenergetic profiling as a novel anti-mycobacterial drug screen.** Dirk A. Lamprecht, Bridgette M. Cumming and Adrie J.C. Steyn
7. **2<sup>nd</sup> H3-D Symposium: Innovative Approaches to Tuberculosis Drug Discovery.** 27-29 August 2014, Victoria Falls, Zambia. **Real time mycobacterial bioenergetic profiling as a novel anti-mycobacterial drug screen.** Dirk A. Lamprecht and Adrie J.C. Steyn.

8. **2<sup>nd</sup> H3-D Symposium: Innovative Approaches to Tuberculosis Drug Discovery**, 27-29 August 2014, Victoria Falls, Zambia. *Redirecting energy metabolism as a strategy for antimycobacterial drug discovery*. Adrie JC Steyn.

**7. INVENTIONS, PATENTS AND LICENSES:** Nothing to report.

**8. REPORTABLE OUTCOMES:** We report the use of a fully integrated, multi-well instrument (Seahorse XF96 metabolic flux analyzer; Seahorse Biosciences, MA) located in our BSL3 facility that non-invasively performs real-time measurements of OCR and ECAR every 2 to 5 minutes. *To date, this technology has not yet been applied to study the bioenergetics of microorganisms. We have successfully adapted this technology for studying bioenergetic changes in Mycobacterium tuberculosis and in Mtb-infected mouse and human cells.*

**9. OTHER ACHIEVEMENTS:** Nothing to report

**10. REFERENCES:** None required